Enzyme-assisted glucose quantification for a painless Lab-on-PCB patch implementation

Gorachand Dutta[a,b], Anna Regoutz[c], Despina Moschou[a,*]

[a]Centre for Biosensors, Bioelectronics and Biodevices (C3Bio), Department of Electronic & Electrical Engineering, University of Bath, Bath BA2 7AY, UK

[b] Currently with: School of Medical Science and Technology (SMST), Indian Institute of Technology Kharagpur, Kharagpur, West Bengal 721302, India

[c]Department of Chemistry, University College London, 20 Gordon Street, London WC1H 0AJ, UK

*Corresponding author. Tel.: +44 (0) 1225 383245;

E-mail address: d.moschou@bath.ac.uk.

Abstract

In the context of an integrated Lab-on-PCB wearable patch extracting interstitial fluid from the patient via integrated microneedles, the requirements from the integrated biosensing part are quite special compared to static glucose electrochemical biosensors. Hence, in this study, a fully PCB-integrated enzymatic glucose quantification Lab-on-Chip device is presented and evaluated considering these special requirements for such a patch implementation: a) range and limit of detection compatible with interstitial fluid glucose levels of diabetic patients and b) effect of sample flow rate on the biosensing platform performance. This work employs a chronoamperometric approach for glucose detection based on covalently immobilized glucose

oxidase on PCB-integrated electrodes. The chronoamperometric measurements show that this platform exhibits μM range sensitivity, high specificity, and good reproducibility, and the assay can detect glucose from 10 μM to 9 mM with a lower limit of detection of 10 μM. The demonstrated detection range under continuous flow proved compatible with interstitial fluid glucose levels of diabetic patients. The sample-to-answer time of our Lab-on-PCB device is less than one minute (sample delivery of few seconds and 20 sec for electrochemical measurement), employing sample volumes of 50 μL in this instance. Increased flow rates substantially improve the platform sensitivity (1.1 μA/mM @0μL/min to 6.2 μA/mM @10μL/min), with the measured current increasing exponentially to the flow rate, as opposed to the theoretically expected much lower dependence. This work demonstrates the feasibility of Lab-on-PCB patches in terms of biosensing performance, paving the way for the first cost-effective, painless diabetes management microsystem.

Keywords: Glucose; Lab-on-PCB; microfluidics; flow rate dependence; chronoamperometry; electrochemical biosensor

1. Introduction

Diabetes is a lifelong condition that causes a person's blood sugar level to increase beyond healthy levels (Breton et al., 2013; Knutsson and Kempe, 2014). It is very important for diabetes to be diagnosed as early as possible as it gets progressively worse if left untreated. A particular concern is that recently diabetes rates have been rising rapidly in low- and middle-income countries (Arredondo et al., 2018; Aziz et al., 2018; Dagenais et al., 2016; Owolabi et al., 2018). Blood glucose diagnostics predominantly based on electrochemical biosensors at the point-of-care are widely available on the market. However, invasive finger pricking is almost always required to collect the necessary blood sample. Non-invasive diagnostic systems are expensive (ca. £60 per sensor) and thus cannot be easily adopted by healthcare systems or accessed by patients in low and middle income countries for routine glucose monitoring.

To this end, our work focuses on the development of a cost-effective electrochemical glucose quantification microsystem, compatible with minimally invasive and thus painless sample extraction devices, such as hydrogel microneedle arrays. This type of array is able to attach to the skin of the patient and continuously extract μL volumes of interstitial fluid (ISF). The glucose concentrations in ISF is proportional to the blood levels, but are at much lower absolute levels (μM as opposed to mM range in whole blood). The real-life implementation of such a device necessitates the following requirements: (a) a passive (pump-less) system continuously extracting the sample from the microneedle array, (b) a biosensing system quantifying the glucose content of ISF under continuous flow, within the respective clinical range, and (c) a cost-effective, mass-manufacturable flexible microsystem seamlessly integrating all the previous functionalities.

In order to realize these requirements, our designed biosensing platform is fabricated via flexible printed circuit board (FPC) technology, ensuring cost-effective upscaling of the patch. An innovative solution is proposed to extract and deliver the interstitial fluid from the needles to the glucose sensors, exploiting passive microfluidics (Vasilakis, 2016). Our designed Lab on Printed Circuit Board (Lab-on-PCB) system (van den Berg, 1998) integrates sample delivery microfluidics and sensitive electrochemical biosensing in a seamlessly fabricated, single platform, furthermore enabling easy integration of electronics for data acquisition and transmission. The device also addresses the requirement for cost-effective mass manufacturing (Jolly et al., 2019; Moschou and Tserepi, 2017), with a projected mass-manufacturing cost for the integrated device of below $1.

This work focuses on the biosensing part of the patch, studying its performance in order to meet the requirement to quantifying the glucose content of ISF under continuous flow, within the respective clinical range. A small number of examples of PCB integrated electrochemical glucose biosensors exist, however, their performance characteristics are not studied for an ISF-focused application or under continuous flow conditions and thus are not suitable for a wearable microsystem implementation (Pu et al., 2016; Jamaluddin et al., 2017; Kassanos et al., 2018; Li et al., 2013; Moschou et al., 2016). Here we report for the first time a fully integrated PCB-implemented electrochemical glucose biosensing microsystem that can detect μM levels of glucose within the interstitial fluid clinical range. The effect of different sample flow rates on the sensor performance is explored in order to identify the flow rate requirement for a subsequent passive microfluidic implementation.

2. Experimental

2.1. Reagents

Acetone, ethanol, ammonium hydroxide (NH_4OH), hydrogen peroxide (H_2O_2), dimethyl sulfoxide (DMSO), 3-mercaptopropionic acid (MPA), N-(3-dimethylaminopropyl)-N′-ethylcarbodiimide hydrochloride (EDC), N-hydroxysuccinimide (NHS), glucose oxidase (GOx, type x-s from Aspergillus niger), ascorbic acid, uric acid, fructose, phosphate-buffered saline (PBS, pH 7.4) and all reagents for buffer solutions were obtained from Sigma-Aldrich, UK. All buffer solutions were prepared using (deionized) DI water (18.3 $M\Omega.cm^{-1}$).

2.2. Design of Lab-on-PCB for glucose sensing

The Lab-on-PCB device was designed in a standard PCB design CAD software (Altium Designer®). It comprises two layers: a gold plated sensing electrode layer, housing the sensing electrodes, and a microfluidic layer including the sample delivery microfluidic channels (Jolly et al., 2019). The device was commercially fabricated in a standard PCB manufacturing facility (Lyncolec Ltd, Poole, UK). The copper electrodes were electroplated with a hard-gold finish in order to exploit the pore-free deposition and low contact resistance achieved by this technique. The sensing electrode layer comprises four identical groups of electrodes, enabling the simultaneous detection of four different analytes in parallel. Each of these groups houses gold-plated electrodes of different shapes, connected electrically by the user at will in order to realize the sensing configuration of choice. In this work, the 1.1mm diameter circular gold-plated electrodes were exploited as working (WE) and pseudo-reference (pseudo-RE) electrodes, while the 1.1mm wide crescent-shaped electrode was used as a counter electrode (CE). The electrodes were connected via the board PCIe slot-type interface to a potentiostat to obtain the cyclic voltammograms and chronoamperometric signals.

For continuous flow experiments, the fluidic layer was adhered on top of the sensing layer to form the complete Lab-on-PCB platform. The main fluidic layer comprises a thin FR4 (flame retardant 4) layer to allow for fluidic optical inspection, laminated with a 40 μm thick photopatternable dry film photoresist (DFR). The resist is patterned via conventional photolithography and development in mild basic solution (1% sodium carbonate). The developed fluidic structure is subsequently post-baked for approximately 2 hours to assure DFR solvent evaporation. A custom adhesive layer was employed to form the final stack, laminating a 50 μm thick PMMA film with 3M 468MP acrylic adhesive; the adhesive layer was laser micromachined following the fluidic layer pattern and then pressed at room temperature between the fluidic layer and sensing layer to achieve leak-tight sample flow. The sensing layer consists of two vias at the beginning and end of the microfluidic channel, used as the fluidic inlet and outlet respectively.

2.3. Sensor Preparation

The gold-plated electrodes were cleaned prior to GOx immobilization by subsequent 15 min ultrasonication in acetone, ethanol, and water, followed by 30 min ultrasonication in a solution containing 5:1:1 water, ammonium hydroxide (20%), and hydrogen peroxide (30%). A self-assembled monolayer (SAM) of 3-mercaptopropoinic acid (MPA) was formed on the precleaned PCB gold working electrode surface by dropping 2 μL of DMSO solution containing 1 mM MPA on the surface for 1 h at room temperature (RT, 25 °C) followed by thoroughly rinsing with DMSO and DI water and drying with N_2 gas as previously reported with slight modification (see Fig.1 for a schematic of the covalent immobilization of GOx on the gold PCB surface) (Hwa and Subramani, 2015). 2 μL of 2 mM EDC and 5 mM NHS solution mixture was incubated for 50 min on the electrode surface at RT to activate the carboxylic acid group (-COOH) of the

SAM. The electrodes were then washed twice with PBS. 5 µL of PBS containing 5 mg/mL GOx was dispensed onto the electrode andincubated overnight at 4 °C. The electrodes were then washed twice with PBS and stored at 4 °C.

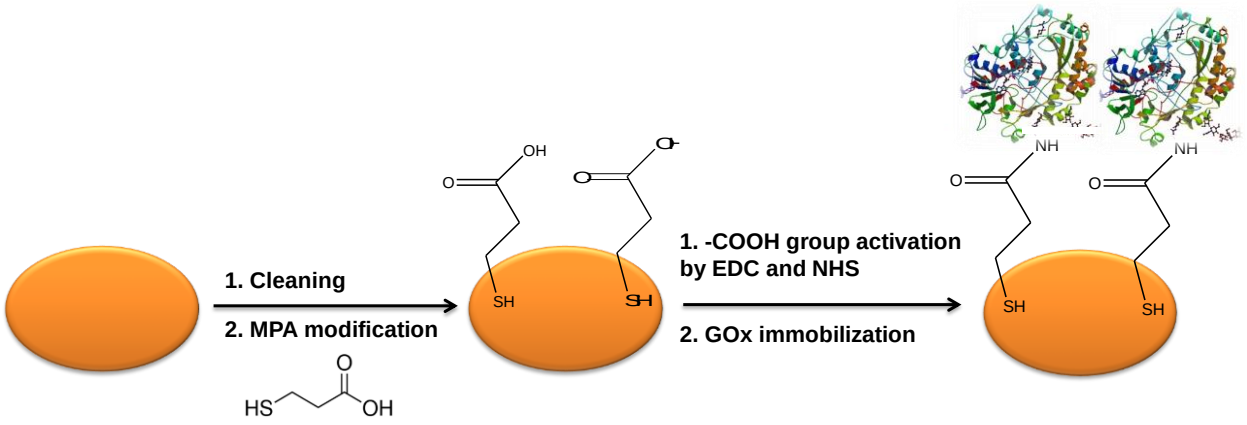

Fig. 1. Schematic illustration of covalent immobilization of GOx on gold PCB surface.

2.4. Experimental Setup and Electrochemical Measurements

100 mM glucose was prepared in 0.1 M PBS solution and stored overnight at RT to mutarotate the α-D-glucose ⇌ β-D-glucose. Different concentrations of glucose samples were prepared by serially diluting the 100 mM stock solution in 0.1 M PBS solution. A 60 µL glucose sample was dispensed onto the sensor and cyclic voltammetric/chronoamperometric measurements were performed using an electrochemical workstation (Autolab, Netherlands). For continuous flow experiments, the glucose samples were delivered via a syringe pump (Cole Palmer 230-CE) into the Lab-on-PCB inlet and waste glucose solution was collected through the fluidic outlet into a beaker. Interfacing fluidic tightness was achieved via a custom-made PMMA chip holder, housing Upchurch® polymer microfluidic ports and ferrules. All electrochemical data were obtained at RT. The cyclic voltammograms were performed in a three-electrode

configuration cycling the potential between −0.3 V and 0.3 V (scan rate: 0.05 $Vsec^{-1}$). The chronocoulometric measurements were recorded by the application of a 0.25 V bias potential exposed in different glucose concentrations in PBS.

2.5 X-ray Photoelectron Spectroscopy

X-ray Photoelectron Spectroscopy (XPS) was performed to investigate the oxidation sate of Au and Cu. A Thermo Scientific K-Alpha+ spectrometer with a monochromated, microfocused Al Kα X-ray source (hυ = 1486.6 eV) was used. The system operates at a base pressure of 2×10-9 mbar and an X-ray spot size of 400 μm was used. Samples were mounted using conducting carbon tape and a flood gun was used to minimize sample charging. Data were collected at 200 eV pass energy for survey and 20 eV pass energy for core level spectra. All data were analyzed using the Avantage software package.

3. Results and Discussion

3.1 Characterization of the PCB Surface

Thorough characterization of the PCB electrode surface was performed, starting with the electrochemical characterization before (BC) and after (AC) the cleaning of the PCB electrode surface. The gold-plated PCB electrodes are completely electrochemically inactive before cleaning and show no oxidation or reduction peaks in the cyclic voltammogram of $K_3Fe(CN)_6$ solution (see Fig. 2a). After the cleaning process, the anticipated oxidation and reduction peaks are clearly observed in cyclic voltammograms. An obvious conclusion is that that the presence of an overlayer of e.g. organic species covering the working area of the electrode of the industrial PCB substrates hinders the transfer of redox species to the gold electrode surface.

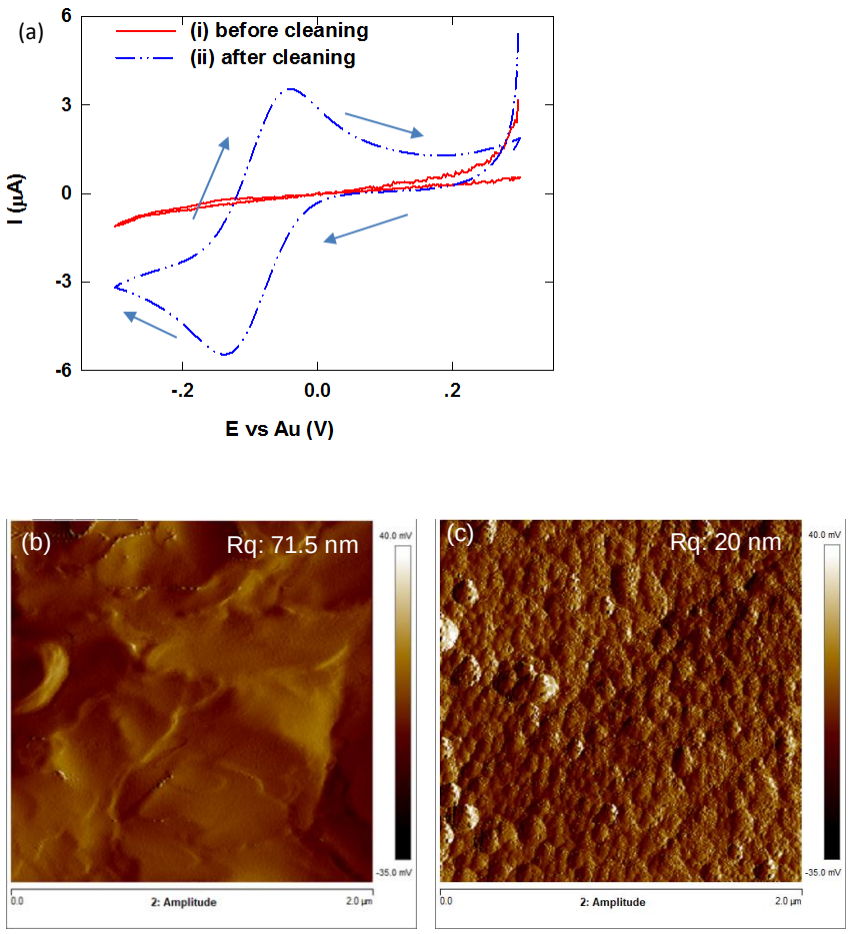

Fig. 2. (a) Cyclic voltammograms recorded at a scan rate of 50 mV/s in a PBS solution containing 4 mM $K_3Fe(CN)_6$ (i) before PCB cleaning and (ii) after cleaning PCB cleaning. (b)-(c) 2 × 2 μm^2 AFM images of the PCB gold surfaces before cleaning (b) and after cleaning (c). Values for the root mean square roughness Rq are given for each image.

To further investigate this, X-ray photoelectron spectroscopy (XPS) and atomic force microscopy (AFM) of the PCB electrode surfaces were performed before and after cleaning. The XPS survey spectra (see Fig. 3(a)) show that before cleaning the surface is almost entirely covered by an organic overlayer of C and O and the curved background shape is typical for the presence of such an overlayer. After cleaning a large proportion of the overlayer is removed and

the spectrum exhibits the expected Au signals as well as core levels from Cu. From detailed core level spectra, information about the chemical state can be extracted (see Figure 3(b)-(d)). The Au 4*f* core level (see Fig. 3(b)) is at a binding energy typical for its metallic state (84.1 eV) both before and after cleaning. Copper could not be detected before cleaning due to the overlayer present and the relatively smaller signal intensity compared to gold. After cleaning the Cu $2p_{3/2}$ core level (see Fig. 3(d)) is found at a binding energy of 932.4 eV. This position indicates the presence of Cu in either the 0 or +1 oxidation state. There is only a minimal chemical shift between these two oxidation states of copper in the Cu $2p_{3/2}$ core level and therefore they cannot be differentiated from the core level alone. However, the presence of Cu^{+1} can be excluded based on the observed O 1*s* core level (see Fig. S1(a) in the Supplementary Information). The only possible Cu^{+1} compound that could be present based on the elements detected in the survey spectrum, is Cu_2O. However, no signal is found for the corresponding O 1*s* feature, which should be located at a binding energy of around 530.5 eV (the lowest feature in the O 1*s* spectrum is at a considerably higher binding energy of 531.3 eV). Therefore, Cu after cleaning is present in its metallic state. Finally, the C 1*s* core level shows a main contribution at 284.8 eV typical for predominantly aliphatic species. From peak fits to the core level spectra relative atomic ratios could be determined (see Fig. S1(b)). As obvious from the survey spectra before cleaning the surface is almost completely dominated by carbon, whilst after cleaning a ratio of 1:1 of Au : C is found. In addition to this change, a considerable signal from Cu is observed after cleaning resulting in a ratio of 78.7 : 21.3 rel. at.% of Au : Cu is found. AFM was used to investigate the surface morphology of the electrodes (see Fig. 2 (b)-(c)), where a clear change in overall appearance is observed after cleaning. Before cleaning the samples show a dune like structure of the organic overlayer with a high surface root mean square roughness Rq of 71.5 nm. After

cleaning the typical island-like microstructure of a deposited metal surface becomes visible and the overall Rq decreases to 20.0 nm.

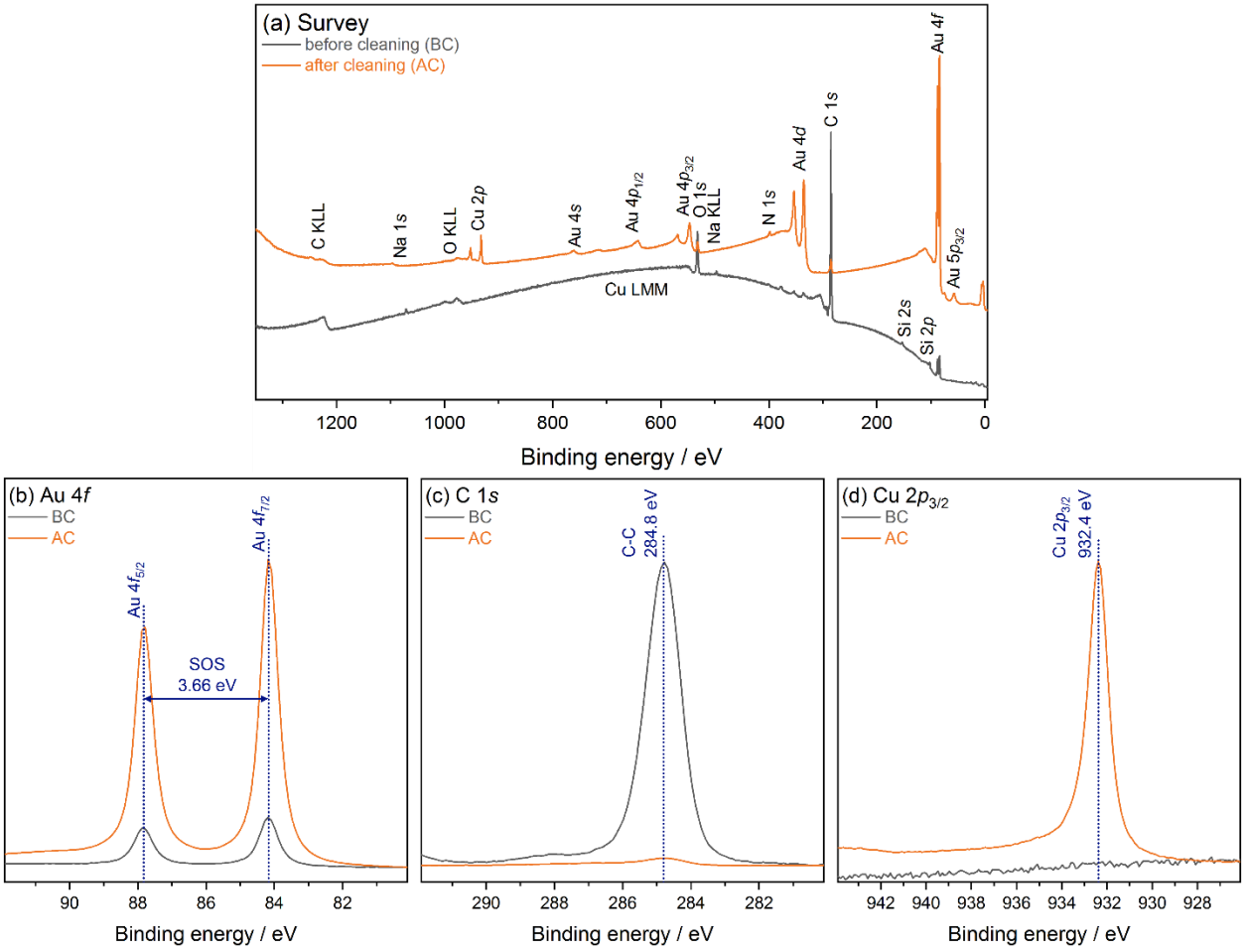

Fig. 3. XPS results of the PCB surface before (BC) and after (AC) cleaning, including (a) survey spectra, and (b)-(d) the Au 4*f*, C 1*s* and Cu $2p_{3/2}$ core level spectra.

3.2. Description of the Detection Scheme and Glucose Measurement

Illustrations of the immobilization procedure of GOx in this detection scheme are shown in Fig. 1. Three consecutive cyclic voltammograms were performed cycling the potential between −0.3 V and +0.3 V at a scan rate of 0.05 $Vsec^{-1}$ on the GOx immobilized PCB surface in 0.1 M PBS

solution to remove the loosely bound GOx from the PCB electrode surface. The chemical binding of the GOx on the PCB surface was characterized by performing cyclic voltammograms in 0.1 M PBS containing 5 mM glucose (Fig. S2 (a)). Chemically immobilized GOx PCB electrode surfaces show a higher oxidation and reduction current (curve i of Fig. S2 (a)) than non-immobilized PCB electrode surfaces (curve ii of Fig. S2 (a)), thus clearly demonstrating that GOx was successfully immobilized on the PCB electrode surface. Fig. S2 (b) shows the GOx chemical binding on the PCB surface in the absence of glucose.

Experiments were carried out to investigate the glucose detection performance of the chemically immobilized GOx PCB surface. Chronoamperometric measurements performed after 60 µL of glucose sample was drop cast on the electrode surface, followed by the application of a 0.25 V bias potential. The chronoamperometric response profiles from 10 µM to 9 mM are shown in Fig. 4a. A calibration plot of the chronoamperometric current at 20 sec is shown in Fig. 4b where each data point represents three separate measurements using new sensors. The electrochemical current was not linearly proportional to the glucose concentration within the complete studied range as the sensitivity of the sensor was higher for lower concentrations (ISF range). Based on these results, this biosensor exhibits a lower limit of detection (LOD) of 10 µM. The detection limit was calculated first by determining 3× the standard deviation (SD) of the signal at zero concentration which is represented by the dashed line in Fig. 4b. The limit of detection is defined as the lowest detectable concentration above the +3SD line. This assay also exhibits highly accurate and reproducible measurements with the Coefficient of Variation less than 8 %.

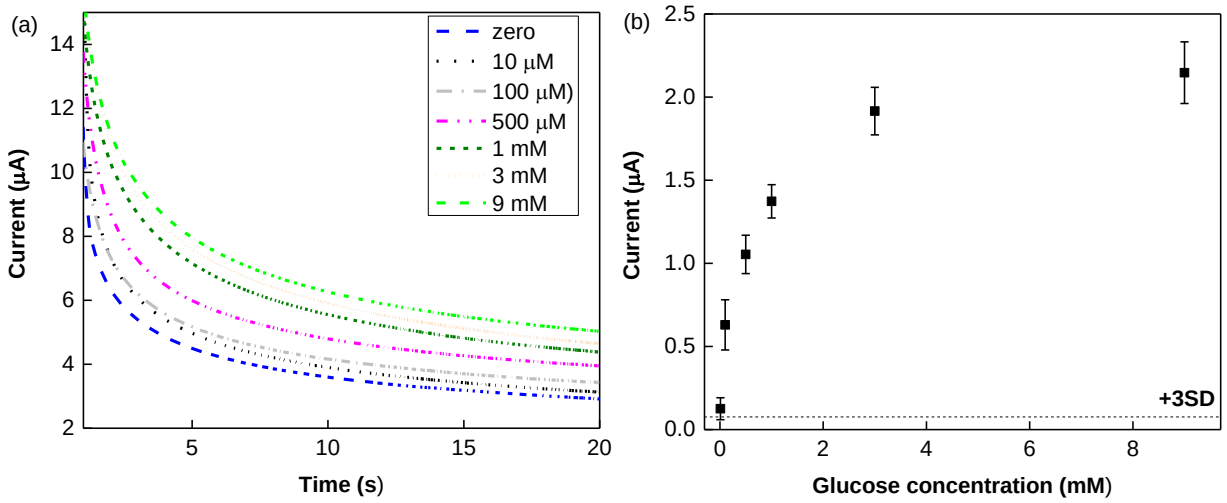

Fig. 4. (a) Amperometric response of chemically immobilized GOx modified PCB biosensor with 0-9 mM glucose in PBS. (b) Calibration plot of glucose concentration based on chronoamperometric currents at 20 s from the response profile in panel a. Each data point represents the mean ± SD of three separate measurements obtained using new sensors.

In order to verify the specificity of the biosensor to glucose, chronoamperometric measurements of PBS samples containing 1 mM glucose or common interfering species, including fructose, uric acid, and ascorbic acid were performed. The signals obtained from fructose, uric acid or ascorbic were comparable with the signal obtained from PBS only (see Fig. S3 in the Supplementary Information). In contrast, the detection signal for glucose was significantly higher then those from interfering species and consistent with our prior glucose detection data (Dutta et al., 2018). The present results suggest that this glucose biosensor is highly specific toward glucose and will not suffer from interference with other species or isomers that may be present in real interstitial fluid samples.

3.3. Flow test with fully integrated microfluidic system

In the next step of this work, a fully integrated Lab-on-PCB microsystem, including the sample delivery microfluidics, was designed to address the sample handling requirements of a final glucose sensing patch analyzing patient samples under constant flow. The device was interfaced via a custom-made PMMA chip holder (see Fig. 5a), housing commercially available fluidic ports and ferrules to deliver the glucose sample from the syringe into the microfluidic inlet and collect the waste from the outlet. The syringes were filled with varying concentrations of glucose, including 10 µM, 100 µM, and 1 mM, and were injected into the Lab-on-PCB device via the microfluidics under a constant flow rate. The effect of different flow rates of 1, 5, and 10 µL/min in this integrated Lab-on-PCB microsystem was investigated with each glucose solution with varying concentrations injected continuously throughout the chronoamperometric measurements. After each measurement the sensing surface was thoroughly rinsed to remove any excess glucose with a PBS injection for 5 min under a constant flow rate of 10 µL/min (50 µL total volume) and the same sensing surface was used for a subsequent glucose sample injection with a larger glucose concentration. The chronoamperometric currents were recorded in a three-electrode configuration and are shown in Fig. 5 (b).

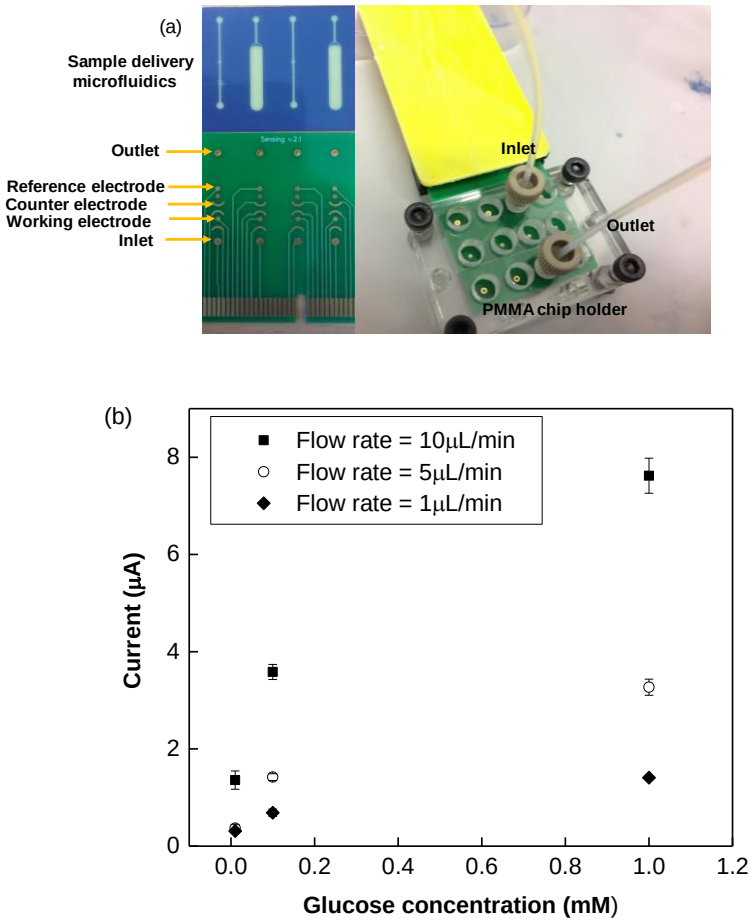

Fig. 5. (a) Illustration of the fully integrated Lab-on-PCB microsystem for the electrochemical glucose detection with commercially fabricated PCB including sample delivery microfluidics. A custom-made PMMA chip holder was interfaced with the device, housing commercially available fluidic ports and ferrules to deliver the glucose sample from the syringe into the microfluidic inlet and collect the waste from the outlet. (b) Chronoamperometric current recordings in a three-electrode configuration for 10 µM, 100 µM, and 1 mM glucose samples under a constant flow rate.

As theoretically anticipated (Kim et al., 2013), the current increases with the flow rate compared to static operation (Fig. 6a) and the detection limit improves with 10 µL/min flow rate (ΔI = 0.61 µA, LoD = 2 µM) compared to static operation (ΔI = 0.12 µA, LoD = 10 µM) and 1 µL/min flow rate (ΔI = 0.22 µA, LoD = 5 µM). Interestingly, the plot of current versus flow rate (Fig. 6b) did not follow the physical model reported in literature ($y=ax^{1/3}$) but followed an allometric function ($y=a+bx^{c}$) instead, where the exponent is far from the theoretical value of 1/3 (Table 1 in Supporting Information). Hence, in practice the current increases exponentially to the power of two with increasing flow rate, in a much more pronounced manner than anticipated in theory. This observation illustrates the increased importance of incorporating continuous sample flow for high sensitivity analyte quantification.

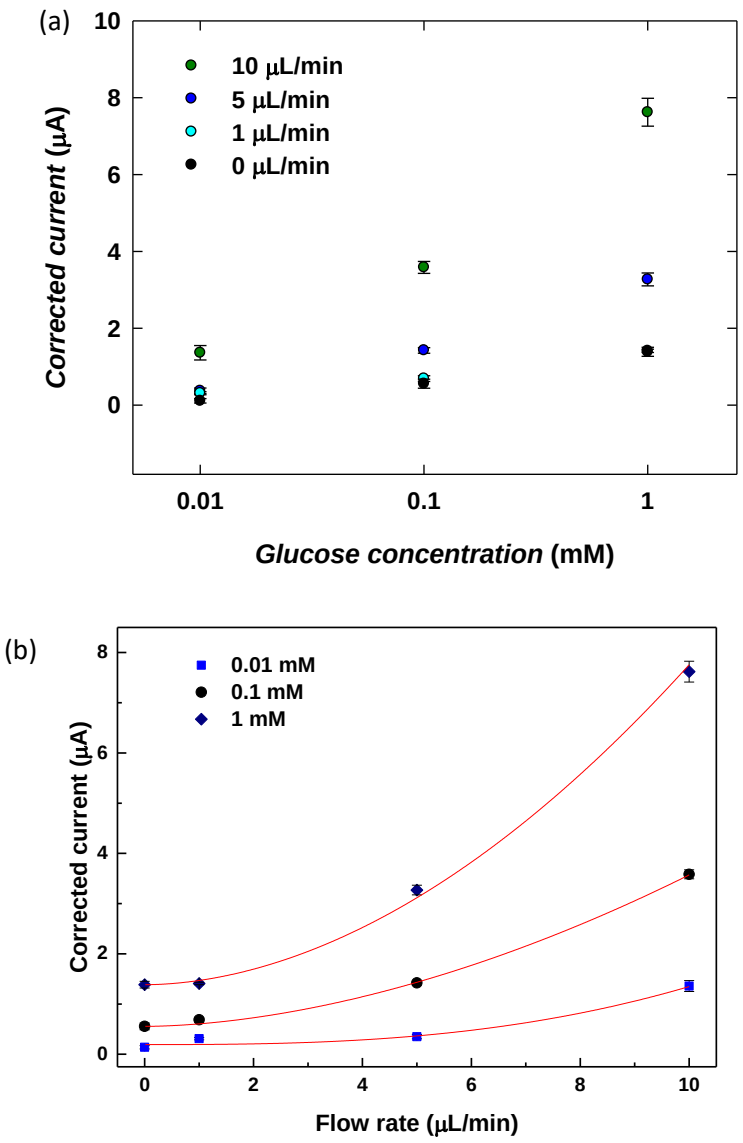

Fig. 6. a) Biosensor calibration curve in semi-logarithmic scale for three different sample flow rates (1 µL/min, 5 µL/min, 10 µL/min) and b) dependence of biosensor recorded current as a function of the sample flow rate, for the three samples of different glucose concentration (0.01 mM, 0.1 mM and 1 mM) and respective fitted curves ($y=a+bx^c$).

4. Conclusions

This paper reports the first fully integrated Lab-on-PCB microsystem for electrochemical glucose quantification using a commercially fabricated PCB base, compatible with a microneedle-based, wearable microsystem implementation. A thorough PCB cleaning process is essential to remove the organic impurity overlayers from the commercially fabricated electrode surfaces to implement biosensors successfully. Chronoamperometric measurements show that the PCB-implemented biosensor exhibits a lower limit of detection of 10 μM in static operation, which is within the clinical range for glucose in interstitial fluid for diabetic patients. The complete Lab-on-PCB microsystem has a much improved glucose sensing behavior when increasing sample flow rates are used. The reported dependence of the recorded current as a function of the squared flow rate is of particular interest and clearly suggests that the use of continuous flow systems is favored when implementing biosensing systems for high sensitivity applications. This works enables the subsequent design of the proposed system in a flexible, cost-effective Lab-on-PCB microneedle patch format, extending it to include the sample extraction microfluidic modules and electronics for signal acquisition and transmission.

Acknowledgements

The authors wish to acknowledge the financial support of British Council (Newton Fund Institutional Links, UK-Turkey project: 336872) and also thank the Spirit Circuits Group and Lyncolec Ltd for their collaboration in manufacturing the prototypes. AR acknowledges the support from Imperial College London for her Imperial College Research Fellowship. GD acknowledges support from ISIRD at IIT Kharagpur.

References

Aracil, C., Perdigones, F., Moreno, J.M., Luque, A., Quero, J.M., 2015. Microelectron. Eng. 131, 13-18.

Arredondo, A., Orozco, E., Duarte, M.B., Cuadra, M., Recaman, A.L., Azar, A., 2018. Glob Public Health 14(2), 227-240.

Aziz, Z., Mathews, E., Absetz, P., Sathish, T., Oldroyd, J., Balachandran, S., Shetty, S.S., Thankappan, K.R., Oldenburg, B., 2018. Implement Sci. 13(1), 97.

Breton, M.C., Guénette, L., Amiche, M.A., Kayibanda, J.F., Grégoire, J.P., Moisan, J., 2013. Diabetes Care 36(3), 740-749.

Dagenais, G.R., Gerstein, H.C., Zhang, X., McQueen, M., Lear, S., Lopez-Jaramillo, P., Mohan, V., Mony, P., Gupta, R., Kutty, V.R., Kumar, R., Rahman, O., Yusoff, K., Zatonska, K., Oguz, A., Rosengren, A., Kelishadi, R., Yusufali, A., Diaz, R., Avezum, A., Lanas, F., Kruger, A., Peer, N., Chifamba, J., Iqbal, R., Ismail, N., Xiulin, B., Jiankang, L., Wenqing, D., Gejie, Y., Rangarajan, S., Teo, K., Yusuf, S., 2016. Diabetes Care 39(5), 780-787.

Debebe, A., Temesgen, S., Redi-Abshiro , M., Chandravanshi, B. S., Ele, E., 2018. J. Anal. Methods. Chem. 2018, 2018, 1-10.

Dutta, G., Regoutz, A., Moschou, D., 2018. Proceedings, 2(13), 741.

Economou, A., Kokkinos, C., Prodromidis, M.,2018. Lab Chip 18(3), 1812-1830.

Guo, J., 2017. Anal.Chem. 89, 8609-8613.

Guo, J., Li, C.-M., Kang, Y., 2014.Biomed. Microdevices 16(5), 681-686.

Guo, J., Ma, X.,2017.. Biosens. Bioelectron. 94, 415-419.

Huang, Z., Yang, J., Zhang, L., Geng, X., Ge, J., Hu, Y., Li, Z., 2017. Anal. Methods. 9, 4275-4281.

Hwa, K.-Y. Subramani, B., 2015. J Med Biol Eng 4, 297-301.

Jamaluddin, A., Taufik, U., Iriani, Y., Budiawanti, S., Suyitno, 2017.. AIP Conf. Proc. 1788, 030092-1-030092-5..

Jolly, P., Rainbow, J., Regoutz, A., Estrela, P., Moschou, D., 2019. Biosens. Bioelectron. 123, 244-250.

Kassanos, P., Anastasova, S., Yang, G.-Z., 2018. IEEE SENSORS, New Delhi, 1-4.

Kim, T.-H., Abi-Samra, K., Sunkara, V., Park, D.-K., Amasia, M., Kim, N., Kim, J., Kim, H., Madou, M., Cho, Y.-K., 2013. Lab Chip 13, 3747-3754.

Knutsson, A., Kempe, A., 2014. Chronobiol. Int. 31(10), 1146-1151.

Li, X., Zang, J., Liu, Y., Lu, Z., Li, Q., Li, C.M., 2013., Anal. Chim. Acta 771, 102-107.

Litinskaia, E.L., Bazaev, N.A., Pozhar, K.V., Grinvald, V.M., 2017. IEEE Conference of Russian Young Researchers in Electrical and Electronic Engineering (EIConRus), St. Petersburg, 47-49.

Mahato, K., Srivastava, A., Chandra, P., 2017. Biosens. Bioelectron. 96, 246-259.

Moschou, D., Morgan, H., Prodromakis, T., 2016. The 20th International Conference on Miniaturized Systems for Chemistry and Life Sciences (mTAS), Dublin, 0115.

Moschou, D., Tserepi, A., 2017. Lab Chip 17(8), 1388-1405.

Owolabi, M.O., Yaria, J.O., Daivadanam, M., Makanjuola, A.I., Parker, G., Oldenburg, B., Vedanthan, R., Norris, S., Oguntoye, A.R., Osundina, M.A., Herasme, O., Lakoh, S., Ogunjimi, L.O., Abraham, S.E., Olowoyo, P., Jenkins, C., Feng, W., Bayona, H., Mohan, S., Joshi, R., Webster, R., Kengne, A.P., Trofor, A., Lotrean, L.M., Praveen, D., Zafra-Tanaka, J.H., Lazo-Porras, M., Bobrow, K., Riddell, M.A., Makrilakis, K., Manios, Y., Ovbiagele, B., 2018. Diabetes Care 41(5), 1097-1105.

Pu, Z., Wang, R., Wu, J., Yu, H., Xu, K., Li, D., 2016. Sens. Actuators B Chem. 230, 801-809.

Soni, A., Jha, S. K., 2015. Biosens. Bioelectron. 67, 763-768.

van den Berg, A., Lammerink, T.S, 1998. Micro Total Analysis Systems: Microfluidic Aspects, Integration Concept and Applications, in: Manz, A., Becker, H. (eds), Microsystem Technology in Chemistry and Life Science. Springer, Berlin, pp. 21-49.

Vasilakis, N., Moschou, D., Carta, D. Morgan, H., Prodromakis, T., 2016. Appl. Surf. Sci. 368, 69-75.